Article

A triple–helix molecular switch electrochemical ratiometric biosensor for ultrasensitive detection of nucleic acids

Erhu Xiong, Zhenzhen Li, Xiaohua Zhang, Jiawan Zhou, Xiaoxia Yan, Yunqing Liu, and Jinhua Chen

Anal. Chem., **Just Accepted Manuscript** • DOI: 10.1021/acs.analchem.7b01251 • Publication Date (Web): 14 Aug 2017

A triple–helix molecular switch electrochemical ratiometric biosensor for ultrasensitive detection of nucleic acids

Erhu Xiong, Zhenzhen Li, Xiaohua Zhang*, Jiawan Zhou, Xiaoxia Yan, Yunqing Liu and Jinhua Chen*

State Key Laboratory of Chemo/Biosensing and Chemometrics, College of Chemistry and Chemical Engineering, Hunan University, Changsha, 410082, P. R. China

*Corresponding Author

Tel./Fax: +86 731 88821961. E−mail: mickyxie@hnu.edu.cn (XZ); chenjinhua@hnu.edu.cn (JC).

ABSTRACT: Biomolecular receptors such as nucleic acids that switch between two or more conformations upon binding to a specific target can be used to build specific and sensitive biosensors. In this work, based on the electrochemical dual–signaling ratiometric strategy and triple–helix molecular switch, we developed a selective, reusable, and simple electrochemical DNA (E–DNA) biosensor for target DNA (T–DNA) detection. A hairpin DNA capture probe labeled with methylene blue (MB–DNA) self–assembles on the surface of gold electrode (GE) through Au–S bond, and then a single–strand DNA modified with two ferrocenes (Fc–DNA) on each end to enhance the oxidation signal hybridizes with the MB–DNA to form a triple–helix conformation. When T–DNA exists, the Fc–DNA hybridizes with T–DNA disassembling the triple–helix stem and allowing the MB–DNA to revert to its hairpin structure. Hence, the Fc tags diffuse away from the GE surface while the MB tags remain affixed close to it, resulting in a decrease in the peak current of Fc (I_{Fc}) and an increase in that of MB (I_{MB}). The linear relationship between the value of I_{MB}/I_{Fc} and the T–DNA concentration is observed from 0.5 pM to 80 pM, and the limit of detection (LOD) is as low as 0.12 pM. The developed E–DNA biosensor may have great potential in the electrochemical detection of a wide range of analytes and be a biosensing platform for early clinical diagnosis and biomedical research.

Nucleic acids are large and important biomolecules that encode and regulate the expression of genetic information in all living things.[1] However, some small changes in nucleic acid sequence can result in significant biomedical and biological implications, for instance, human diseases, bacterial drug resistance, and population genetics.[2,3] Therefore, accurate, rapid and specific nucleic acid analysis is important for pathogen detection, clinical diagnosis, and gene therapy. In recent years, various kinds of biosensors have been developed including those based on colorimetry,[4-7] fluorescence,[8-13] electrochemiluminescence,[14-16] photoelectrochemistry,[17-19] dynamic light scattering technique,[20] and electrochemistry.[21-28] Among these DNA biosensors, electrochemical biosensors have attracted substantial attention due to their high sensitivity, simplicity, quick response, low cost, and relatively low power consumption.[29-33]

Recently, based on Hoogsteen and Watson–Crick base pairings, a triple–helix molecular switch has been studies and applied in electrochemical DNA biosensors (E–DNA biosensors).[34–35] For example, Adriana et al. developed a reagentless, electrochemical biosensor for the sensitive detection of double–stranded DNA targets based on a triplex–forming oligonucleotide probe.[35] Wang et al. developed a signal–on and label–free E–DNA biosensor using the triplex DNA structure with a low detection limit.[36] The property of the triple–helix conformation is independent of any particular binding sequence it carries, making the triple–helix biosensing strategy universally applicable. In comparison with the traditional duplex DNA biosensors, the biosensors based on the triple–helix conformation have some unique advantages. For instance, the triple–helix conformation formed via two short–armed complementary oligos of the binding probe has similar stability to the duplex DNA achieved through the design with a longer complementary oligo, and allows more target sequence to be free, thereby enhancing both the specificity and binding affinity to the intended analytes, and even enabling much higher sensitivity.

However, up to now, most electrochemical biosensors based on the triple–helix molecular switch have only one of two types of signal readout: either a "signal–off" or a "signal–on". "Signal–off" biosensors are limited by the capacity of their signal, under any experimental conditions, there is only a maximum of 100% signal suppression can be achieved. Thus, to take advantage of the preponderance of the "signal–on" method and to avoid the drawback of the "signal–off" method, electrochemical ratiometric assays with both "signal–off" and "signal–on" elements have been studied because of their excellent analytical performance (such as low background noise, wide linear range, low detection limit, good reproducibility and reliability).[37-41]

Considering the above findings, by combining triple–helix molecular switch with electrochemical dual–signaling ratiometric strategy, we developed a reusable, selective, and simple E–DNA biosensor for the detection of target DNA (T–DNA) (Scheme 1). A hairpin DNA capture probe labeled with methylene blue (MB–DNA) self–assembles on the gold electrode (GE) surface through Au–S bond, which is then passivated with 6–mercaptohexanol (MCH). Subsequently, a single–strand DNA modified with two ferrocenes (Fc–DNA) on each end to enhance the oxidation signal hybridizes with MB–DNA to form a triple–helix conformation. When T–DNA exists (here, Human Immunodeficiency Virus type 1 (HIV–1) gene is chosen as the model analyte), the loop region of Fc–DNA hybridizes with T–DNA disassembling the triple–helix stem and allowing the MB–DNA to revert to its hairpin structure with the help of Mg^{2+}.[42,43] This causes the Fc tags to be away from the GE surface while the MB tags remain affixed close to it, resulting in a decrease in the peak current of Fc (I_{Fc}) and an increase in that of MB (I_{MB}). The linear relationship between the value of I_{MB}/I_{Fc} and the T–DNA concentration is observed from 0.5 pM to 80 pM, and the limit of detection (LOD) is as low as 0.12 pM. In the sensing system, the combination of dual–signaling strategy and triple–helix conformation makes it effective for dual–label Fc–tags on each end of Fc–DNA, which enhances the Fc signal and the sensitivity of the biosensors. Most importantly, the proposed biosensor is not only selective and sensitive but also convenient, regenerable and universal. Multiple targets (nucleic acids, small molecules, proteins, etc.) can be detected by altering the sequence of Fc–DNA in the loop region without changing MB–DNA and the triple–helix conformation, implying that the developed sensing platform has better extensibility than the previously reported electrochemical dual–signaling ratiometric biosensors and has great potential applications in early disease diagnosis, bioanalysis, and clinical biomedicine.

Scheme 1. Schematic Diagram of the E–DNA Biosensor for the Detection of T−DNA. (a) the Fc–DNA/MCH/MB–DNA/GE, (b) the Fc–DNA/MCH/MB–DNA/GE after treatment with T−DNA.

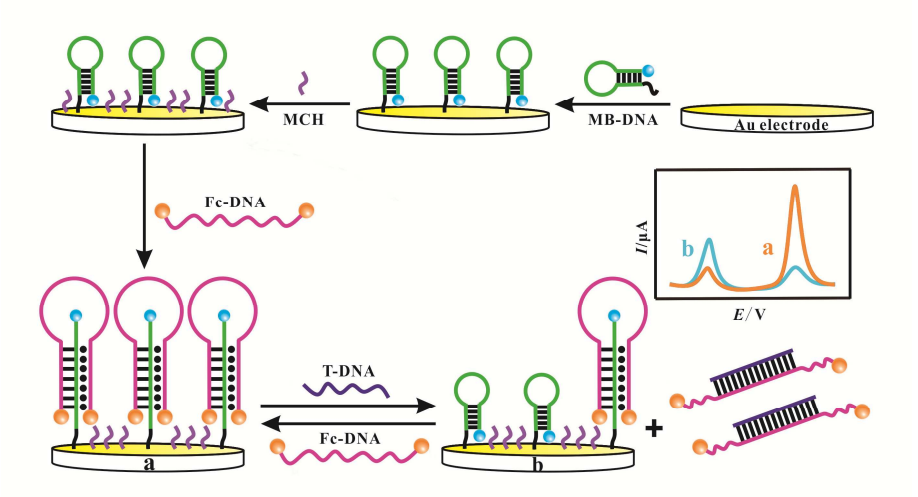

EXPERIMENTAL SECTION

Materials. All HPLC–purified synthetic oligonucleotides used in this work were provided by Sangon Biotech Co., Ltd (Shanghai, China, www.sangon.com). The oligonucleotide sequences were listed in Table S1 (see the Supporting Information). TCEP (tris–(2–carboxyethyl) phosphine) and MCH were supplied by Sigma–Aldrich (Shanghai, China, www.sigmaaldich.com/china). Metal salts (NaCl, $MgCl_2$, KCl, $K_4Fe[CN]_6$, $K_3Fe[CN]_6$, K_2HPO_4, KH_2PO_4) were of analytical grade and purchased from Sinopharm Chemical Reagent Co., Ltd. (Shanghai, China, www.sinoreagent.com). Ultrapure water (>18 MΩ cm, provided by Millipore system (Milli–Q, Millipore, www.merckmillipore.com)) was used throughout. Human serum was obtained from the Affiliated Hospital of Hunan University.

Apparatus. All the electrochemical measurements were carried out using the CHI 660D Electrochemical Workstation (Shanghai Chenhua Instrument Corporation, China, www.chinstr.com) at room temperature, including cyclic voltammetry (CV), electrochemical impedance spectroscopy (EIS), and differential pulse voltammetry (DPV). A conventional three–electrode cell which consisted of a modified GE (2 mm in diameter, working electrode), a platinum wire (auxiliary electrode) and a saturated calomel electrode (SCE, reference electrode) was used in all electrochemical investigations.

Fabrication of the MCH/MB–DNA/GE. At first, the bare GE was polished sequentially with alumina slurries of 0.5 and 0.05 μm, respectively. After that, the bare GE was ultrasonicated in methanol and ultrapure water, followed by the electrochemical pretreatment with potential cycling in 0.5 M H_2SO_4 solution ranging from −0.3 to 1.5 V at a scan rate of 100 mV s^{-1} until a stable cyclic voltammogram was observed. Finally, the bare GE was rinsed with plenty of ultrapure water and dried in a nitrogen stream.

Prior to assembling on the GE surface, the dissolution of the MB–DNA was carried out in 20 mM phosphate buffer solution (PBS, 10 mM TCEP, 2.5 mM $MgCl_2$, 50 mM NaCl, pH 7.4) under darkness for 1 h to decrease disulfide bonds, followed by dropping 20 μL of 1 μM MB–DNA onto the above GE surface and incubating at 25 °C for 16 h to create the MB–DNA/GE. Subsequently, to passivate the free surface of GE as well as to obtain well-aligned DNA monolayers, the MB–DNA/GE was further incubated for 1 h with MCH (2 mM). The resulting electrode was marked as the MCH/MB–DNA/GE. To characterize the stepwise modification process of the electrode interface, electrochemical impedance measurements were carried out in the solution containing 5 mM $[Fe(CN)_6]^{3-/4-}$ and 0.1 M KCl with frequency in the range from 0.1 Hz to 100 kHz, potential at 0.22 V (vs. SCE), and amplitude set at 5 mV.

Electrochemical T–DNA detection. The MCH/MB–DNA/GE was immersed in 20 μL of 20 mM PBS (2.5 mM $MgCl_2$, 0.1 M NaCl, pH 6.0) including 1 μM Fc–DNA at 25 °C for 90 min to form the triple–helix molecular conformation. Subsequently, the resulted Fc–DNA/MCH/MB–DNA/GE was washed thoroughly and incubated with varying concentrations of T–DNA. The electrochemical capability of the resulted electrode was measured with DPV (pulse width, 50 ms; amplitude, 50 mV; sample width, 16.7 ms; pulse period, 200 ms) in 5 mL of 20 mM PBS (50 mM NaCl, 2.5 mM $MgCl_2$, pH 7.4). The control experiments for non–complementary or base–mismatched DNA were also measured under the same conditions. All DPV measurements were performed at 25 °C and at least 3 times.

RESULTS AND DISCUSSION

Characterization of the E–DNA biosensor. As an efficient method for probing the interfacial properties of modified electrodes, EIS is usually carried out to investigate electrode modification by different interfacial processes.[44] In a typical EIS, the section of high–frequency semicircle corresponds to the charge transfer limited process, and an

increment of the semicircle diameter indicates the increase of the resistance of interfacial charge transfer (R_{ct}).[45] As shown in Figure 1, the bare GE exhibits a very small semicircle domain (R_{ct} = 105 Ω, curve a), demonstrating a very fast charge–transfer process. Nevertheless, a large semicircle with R_{ct} value of about 3614 Ω (curve b) can be seen after the immobilization of MB–DNA on the GE surface because of the effective repulsion between $[Fe(CN)_6]^{3-/4-}$ anions and the negatively charged MB–DNA. Subsequently, passivation of the surface with MCH further leads to an evident increase of the R_{ct} value (about 3962 Ω, curve c). The hybridization between Fc–DNA and MB–DNA makes the value of R_{ct} increase to 5876 Ω (curve d), indicating the successful formation of the triple–helix molecular conformation. However, after incubation with T–DNA, the R_{ct} value of the electrode decreases obviously (about 4127 Ω, curve e) because of the hybridization between T–DNA and Fc–DNA and the disintegration of the triple–helix molecular conformation. These results confirm the successful fabrication of the E–DNA biosensor according to Scheme 1.

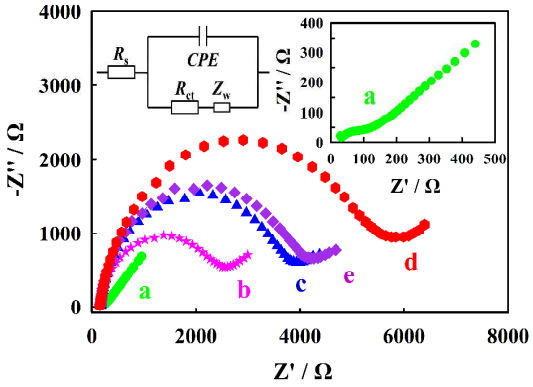

Figure 1. EIS (Nyquist plots) of the different modification process of the electrode interface in the solution containing 5 mM (1:1) $[Fe(CN)_6]^{3-/4-}$ and 0.1 M KCl. Frequency range used for EIS is from 0.1 Hz to 100 kHz; amplitude, 5 mV. Bare GE (a), MB–DNA/GE (b), MCH/MB–DNA/GE (c), Fc–DNA/MCH/MB–DNA/GE (d), Fc–DNA/MCH/MB–DNA/GE after treatment with T–DNA (e). Inset plot in Figure 1 shows the equivalent electrical circuit.

Feasibility of the E–DNA biosensor. DPV investigation was carried out on different modified electrodes in order to further confirm the feasibility of the proposed E–DNA biosensor. After the immobilization of MB–DNA, as shown in Figure 2, there is only a well–defined oxidation peak of MB at approx. −0.3 V due to the efficient electron−transfer of MB molecule (curve a). However, after the MCH/MB–DNA/GE is immersed in PBS with Fc–DNA, there are a significant oxidation peak of Fc (at about 0.35 V) and a small oxidation peak of MB (curve b). Nevertheless, when 30 pM T–DNA is added into the sensing system, the Fc response significantly decreases, whereas the MB response increases (curve c). Based on these results, it clearly reveals that the proposed E–DNA biosensor can be used for the detection of T–DNA.

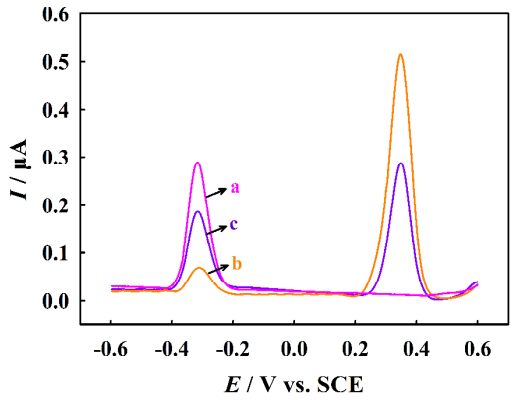

Figure 2. Feasibility of the E–DNA biosensor. DPV responses of MCH/MB–DNA/GE (a), Fc–DNA/MCH/MB–DNA/GE (b), Fc–DNA/MCH/MB–DNA/GE after treatment with 30 pM T–DNA (c).

Optimization of the length of the triple–helix stem. In order to form a triplex conformation via C–G·C^+ and T–A·T base triplets, two-arm sequences of the Fc–DNA were designed to hybridize with the MB–DNA.[46] Based on this design principle, the length of the triple–helix stem is a crucial factor which influences the signal–to–background ratio. It is better to hybridize with MB–DNA with a longer triple–helix stem so that the tighter bind reduces the length of the free region on MB–DNA, resulting in lower background. On the other hand, the release of MB–DNA may be prevented by the longer triple–helix stem, resulting in lower response to the target. Hence, it is necessary to optimize the stem length of the triple helix so as to balance the two competing effects. Four probes with the same recognition sequence as the Fc–DNA were designed, while the two arm sequences varied as 5, 6, 8, and 9 bases, respectively (DNA1, 2, 3, and 4, sequences are listed in Table S1, see Supporting Information). The values of I_{MB}/I_{Fc} of different probes are shown in Figure S1 (see Supporting Information). It is noted that the best efficiency is provided by the probe with 7–base arm sequence, which is in accordance with the previously reported paper.[47]

Optimization of the experimental conditions. It is well known that the stability of the Hoogsteen base pairing is dependent on pH. The Hoogsteen base pairing between C–G·C^+ base triplets under acidic condition can be formed due to the protonation of cytosine residues.[48,49] When pH is raised, the imino group of cytosines cannot be protonated efficiently and the Hoogsteen base pairing becomes unstable so that it is difficult to form the triplex–helix molecular structure. Therefore, in order to ensure the best performance of the proposed E–DNA biosensor, pH is optimized by measuring DPV responses under various pH conditions. As shown in Figure S2A (see Supporting Information), the values of I_{Fc}/I_{MB} initially increase and then decrease with the increase of pH. I_{Fc}/I_{MB} reaches a maximum at pH 6.0. Thus, pH is fixed at 6.0 throughout the experiments.

In addition, reaction time and temperature are also of importance in DNA interaction, and were hence also optimized. As shown in Figure S2B (see Supporting Information), the value of I_{Fc}/I_{MB} increases rapidly with the increase of reaction time and reaches a plateau after 90 min, so

90 min is selected as the optimal reaction time. Meanwhile, the maximum value of I_{Fc}/I_{MB} is observed at 25 °C (Figure S2C (see Supporting Information)), thus, 25 °C is chosen as the optimal temperature for all experiments.

Stabilities of Fc and MB signals and enhancement of Fc signal. In order to evaluate the stabilities of Fc and MB signals, the Fc–DNA/MCH/MB–DNA/GE was measured by continuous DPV scanning. As shown in Figure 3A, there are no obvious changes for the oxidation peaks of Fc and MB during five–time continuous DPV scanning, indicating that the stabilities of Fc and MB signals are satisfactory. In addition, to demonstrate whether the Fc signal is enhanced by using dual–label method, Fc–DNA' with single Fc–tag was designed. As shown in Figure 3B, comparing double Fc–tags (curve a) to single Fc–tag (curve b), the Fc signal has an enhancement of about 80.4%, indicating that the dual–label method has excellent effect on signal enhancement of Fc.

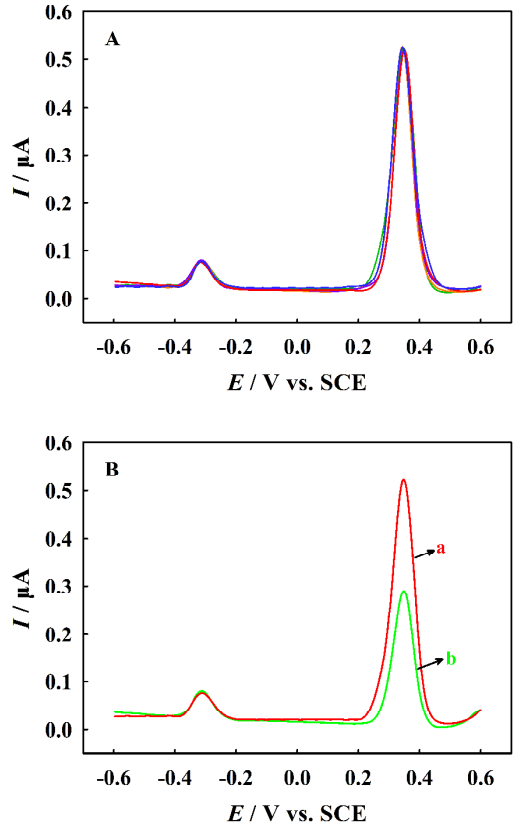

Figure 3. (A) DPV responses of Fc–DNA/MCH/MB–DNA/GE for five–time continuous DPV scanning. (B) DPV responses of Fc–DNA/MCH/MB–DNA/GE (double Fc–tags, curve a) and Fc–DNA'/MCH/MB–DNA/GE (single Fc–tag, curve b).

Electrochemical T–DNA assay. HIV–1 DNA[36,50] was used as the model analyte to verify the applicability of the proposed E–DNA biosensor for quantitative T–DNA detection. Under optimal experimental conditions, a series of T–DNA solutions with different concentrations ranging from 0.5 pM to 300 pM, were measured. As shown in Figure 4A, the MB oxidation peak increases and the Fc oxidation peak decreases with increasing concentration of T–DNA. The calibration curves of the E–DNA biosensor using individual MB signal or Fc signal for T–DNA detection are shown in Figure 4B. Both of them reveal a well–behaved linear relationship between the concentration of T–DNA and the DPV oxidation peak current ranging from 0.5 pM to 50 pM, with LOD values of 0.34 pM (for MB signal) and 0.28 pM (for Fc signal) (S/N = 3), respectively. Furthermore, as shown in Figure 4A, the inset plot also exhibits a linear relationship between the value of I_{MB}/I_{Fc} and T–DNA concentration from 0.5 pM to 80 pM (I_{MB}/I_{Fc} = 0.0232 C_{T-DNA} + 0.0624, R^2 = 0.9845), with a LOD of 0.12 pM (S/N = 3). It is worth noting that the electrochemical ratiometric strategy reveals a wider linear range and a lower LOD than that achieved by using either I_{MB} or I_{Fc} alone. Moreover, to the best of our knowledge, the LOD of our strategy is much lower than that of most other electrochemical strategies, which use only a single response mechanism as the signal.[51-53]

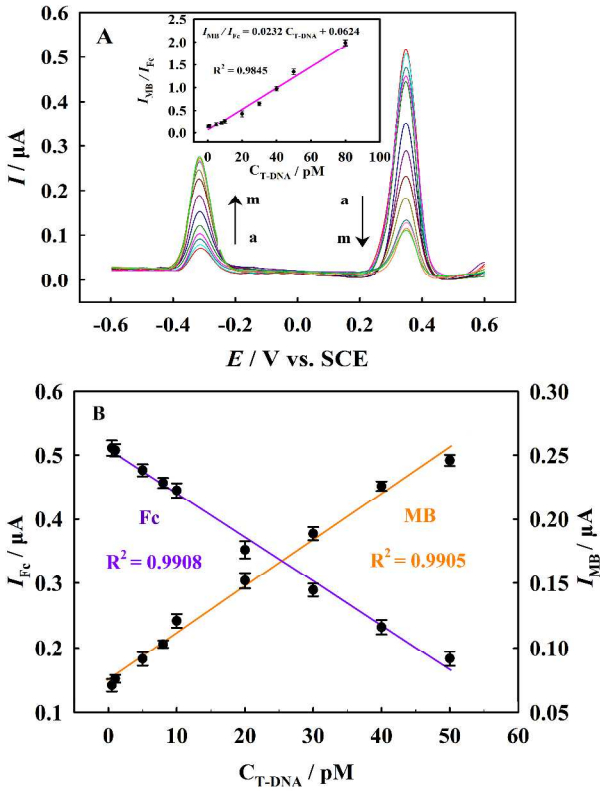

Figure 4. (A) DPV responses to different T–DNA concentrations (a–m: 0.5 pM, 1 pM, 5 pM, 8 pM, 10 pM, 20 pM, 30 pM, 40 pM, 50 pM, 80 pM, 100 pM, 200 pM, 300 pM). Inset: dependence of I_{MB}/I_{Fc} on T–DNA concentration. (B) Calibration curves of I_{Fc} and I_{MB} versus the T–DNA concentrations from 0.5 pM to 50 pM. Error bars stand for the standard deviation of three independent experiments.

Reproducibility, stability, specificity and regeneration of the E–DNA biosensor. The reproducibility of the developed E–DNA biosensor was investigated to ensure its utility for practical applications. Five modified electrodes fabricated under the same procedure were used for the detection of T–DNA (30 pM), and the value of relative standard deviation is found to be 3.7%. The stability of the Fc–DNA/MCH/MB–DNA/GE after refrigerated storage was also tested. As much as 96.2% of its original response to T–DNA in three independent experiments is preserved after the Fc–DNA/MCH/MB–DNA/GE were stored in the fridge at

4 °C for more than 2 weeks. Based on these results, it clearly reveals that the proposed E–DNA biosensor has satisfactory reproducibility and stability.

Furthermore, four kinds of DNA sequences with the same concentration of 50 pM, including non–complementary DNA (N–DNA), three–base mismatched DNA (Tm–DNA), single–base mismatched DNA (Sm–DNA) and T–DNA, have been used to confirm the specificity of the E–DNA biosensor. As shown in Figure 5, the biosensor response due to N–DNA is similar to its response to blank solution. The values of I_{MB}/I_{Fc} toward Tm–DNA and Sm–DNA show only about 25.5% and 47.9% of that toward T–DNA, respectively. In view of these results, the proposed E–DNA biosensor exhibits a satisfactory specificity for T–DNA assay.

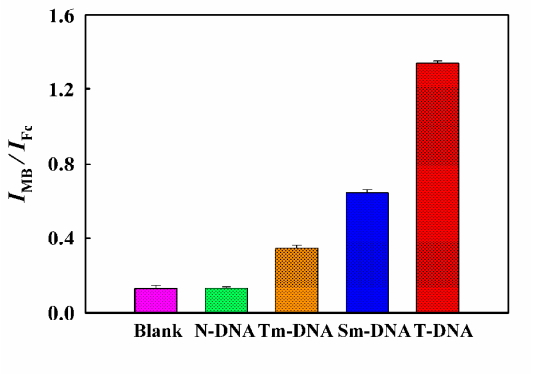

Figure 5. The values of I_{MB}/I_{Fc} for the MCH/MB–DNA/GE in 20 mM PBS with no DNA, N–DNA, Tm–DNA, Sm–DNA, or T–DNA. Error bars stand for the standard deviation of three independent experiments.

In addition, after the T–DNA assay, the E–DNA biosensor can be regenerated easily by incubating the electrode in 20 μL of 1 μM Fc–DNA solution for 90 min. As shown in Figure 6, after five–cycle regeneration, both Fc and MB signals almost fully recover to their initial values, which confirms that the E–DNA biosensor has excellent regeneration ability.

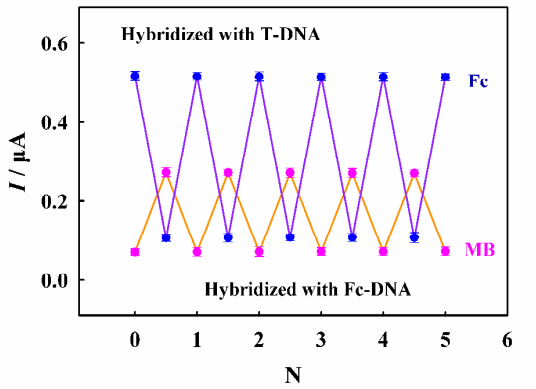

Figure 6. Reversible changes of I_{Fc} and I_{MB} for the regeneration of the E–DNA biosensor under the stepwise hybridization with T–DNA and then with Fc–DNA. N stands for the regeneration times of the biosensor.

Recovery test. To estimate the reliability and applicability of the proposed E–DNA biosensor, the recovery tests for various concentrations of T–DNA have been performed in human serum samples supplied by healthy individuals. As shown in Table 1, various concentrations of T–DNA (0.5 pM, 5 pM, 10 pM, 50 pM) was added into the 10–fold diluted (20 mM PBS) human serum samples, and the recoveries of the added T–DNA are 102.0%, 98.6%, 99.2%, and 101.3%, respectively. In view of these results, the recovery performance of the E–DNA biosensor is quite desirable, implying its great promising application in complex biological samples for T–DNA detection.

Table 1. Recovery tests in diluted human serum samples.

Sample	Added (pM)	Found (pM)	Recovery (%)
1	0.5	0.51 ± 0.03	102.0
2	5	4.93 ± 0.12	98.6
3	10	9.92 ± 0.07	99.2
4	50	50.66 ± 0.21	101.3

CONCLUSION

By combining triple–helix molecular switch with electrochemical dual–signaling ratiometric strategy, we developed a selective, simple, and reusable E–DNA biosensor for T–DNA detection. In comparison with traditional electrochemical biosensors, the developed E–DNA biosensor exhibits excellent stability, sensitivity and selectivity, as well as a lower LOD (0.12 pM, S/N = 3) for T–DNA detection. Moreover, the biosensor could be regenerated readily with basic buffer containing Mg^{2+} without heat-annealing treatment. Critically, the E–DNA biosensor could be easily modified for the detection of arbitrary targets by simply altering its DNA sequence. This generality provides a great potential in bioanalysis, early clinical diagnosis and biomedical research.

AUTHOR INFORMATION

Corresponding Author

*Tel./Fax: +86 731 88821961. E−mail: chenjinhua@hnu.edu.cn; mickyxie@hnu.edu.cn.

Notes

The authors declare no competing financial interest.

ACKNOWLEDGEMENTS

This work was financially supported by NSFC (21475035, 21235002), the Foundation for Innovative Research Groups of NSFC (21521063), Hunan Provincial Innovation Foundation for Postgraduate (CX2016B112), China Scholarship Council (201606130011) and PCSIRT (IRT1238).

Supporting Information

Sequences of oligonucleotides, optimization of stem length of the triple helix and experimental conditions. This material is available free of charge via the Internet at http://pubs.acs.org.

REFERENCES

(1) Sauna, Z. E.; Kimchi−Sarfaty, C. *Nat. Rev. Genet.* **2011**, *12*, 683−691.
(2) Ito, T.; Hosokawa, K.; Maeda, M. *Biosens. Bioelectron.* **2007**, *22*, 1816−1819.

(3) Chen, J. H.; Zhang, J.; Guo, Y.; Li, J.; Fu, F. F.; Yang, H. H.; Chen, G. N. *Chem. Commun.* **2011**, *47*, 8004−8006.
(4) Xu, W.; Xue, X. J.; Li, T. H.; Zeng, H. Q.; Liu, X. G. *Angew. Chem., Int. Ed.* **2009**, *48*, 6849−6852.
(5) Ma, C. P.; Wang, W. S.; Li, Z. X.; Cao, L. J.; Wang, Q. Y. *Anal. Biochem.* **2012**, *429*, 99−102.
(6) Baeissa, A.; Dave, N.; Smith, B. D.; Liu, J. W. *ACS Appl. Mater. Interfaces* **2010**, *2*, 3594−3600.
(7) Zhang, Y. Y.; Tang, Z. W.; Wang, J.; Wu, H.; Maham, A. H.; Lin, Y. H. *Anal. Chem.* **2010**, *82*, 6440−6446.
(8) Li, F.; Du, Z. F.; Yang, L. M.; Tang, B. *Biosens. Bioelectron.* **2013**, *41*, 907−910.
(9) Huang, J. H.; Su, X. F.; Li, Z. G. *Anal. Chem.* **2012**, *84*, 5939−5943.
(10) Hu, R.; Liu, T.; Zhang, X. B.; Huan, S. Y.; Wu, C. C.; Fu, T.; Tan, W. H. *Anal. Chem.* **2014**, *86*, 5009−5016.
(11) Yang, Y.; Zhao, L. X. *TrAC Trends Anal. Chem.* **2010**, *29*, 980−1003.
(12) Liu, G. L.; Li, J. J.; Feng, D. Q.; Zhu, J. J.; Wang, W. *Anal. Chem.* **2017**, *89*, 1002−1008.
(13) Liu, S. F.; Zhang, C. X.; Ming, J. J.; Wang, C. F.; Liu, T.; Li, F. *Chem. Commun.* **2013**, *49*, 7947−7949.
(14) Sun, Q. X.; Zou, G. Z.; Zhang, X. L. *Electroanal.* **2011**, *23*, 2693−2698.
(15) Chai, Y.; Tian, D. Y.; Wang, W.; Cui, H. *Chem. Commun.* **2010**, *46*, 7560−7562.
(16) Zhang, H. R.; Xu, J. J.; Chen, H. Y. *Anal. Chem.* **2013**, *85*, 5321−5325.
(17) Liu, S. L.; Li, C.; Cheng, J.; Zhou, Y. X. *Anal. Chem.* **2006**, *78*, 4722−4726.
(18) Zang, Y.; Lei, J. P.; Zhang, L.; Ju, H. X. *Anal. Chem.* **2014**, *86*, 12362−12368.
(19) Li, C. X.; Wang, H. y.; Shen, J.; Tang, B. *Anal. Chem.* **2015**, *87*, 4283−4291.
(20) Tang, L. H.; Wang, Y.; Liu, Y.; Li, J. H. *Acs Nano* **2011**, *5*, 3817−3822.
(21) Zhang, X. L.; Li, L. L.; Li, L.; Chen, J.; Zou, G. Z.; Si, Z. K.; Jin, W. R. *Anal. Chem.* **2009**, *81*, 1826−1832.
(22) Xiao, Y.; Lou, X. H.; Uzawa, T.; Plakos, K. J.; Plaxco, K. W.; Soh, H. T. *J. Am. Chem. Soc.* **2009**, *131*, 15311−15316.
(23) Hsieh, K.; White, R. J.; Ferguson, B. S.; Plaxco, K. W.; Xiao, Y.; Soh, H. T. *Angew. Chem., Int. Ed.* **2011**, *50*, 11176−11180.
(24) Xiong, E. H.; Yan, X. X.; Zhang, X. H.; Liu, Y. Q.; Zhou, J. W.; Chen, J. H. *Biosens. Bioelectron.* **2017**, *87*, 732−736.
(25) Wu, L.; Xiong, E. H.; Zhang, X.; Zhang, X. H.; Chen, J. H. *Nano Today* **2014**, *9*, 197−211.
(26) Zhang, Y. L.; Wang, Y.; Wang, H. B.; Jiang, J. H.; Shen, G. L.; Yu, R. Q.; Li, J. H. *Anal. Chem.* **2009**, *81*, 1982−1987.
(27) Liu, S. F.; Lin, Y.; Wang, L.; Liu, T.; Cheng, C. B.; Wei, W. J.; Tang, B. *Anal. Chem.* **2014**, *86*, 4008−4015.
(28) Ge, L.; Wang, W. X.; Sun, X. M.; Hou, T.; Li, F. *Anal. Chem.* **2016**, *88*, 9691−9698.
(29) Shu, H. W.; Wen, W.; Xiong, H. Y.; Zhang, X. H.; Wang, S. F. *Electrochem. Commun.* **2013**, *37*, 15−19.
(30) Huang, L. L.; Yang, X. J.; Qi, C.; Niu, X. F.; Zhao, C. L.; Zhao, X. H.; Shangguan, D. H.; Yang, Y. H. *Anal. Chim. Acta* **2013**, *787*, 203−210.
(31) Zhang, B.; Cui, Y. L.; Chen, H. F.; Liu, B. Q.; Chen, G. N.; Tang, D. P. *Electroanal.* **2011**, *23*, 1821−1829.
(32) Xiao, T. F.; Wu, F.; Hao, J.; Zhang, M. N.; Yu, P.; Mao, L. Q. *Anal. Chem.* **2016**, *89*, 300−313.
(33) Xiong, E. H.; Zhang, X. H.; Liu, Y. Q.; Zhou, J. W.; Yu, Peng; Chen, J. H. *Anal. Methods* **2016**, *8*, 2106−2111.
(34) Wang, X. Z.; Jiang, A. W.; Hou, T.; Li, F. *Analyst* **2014**, *139*, 6272−6278.
(35) Patterson, A.; Caprio, F.; Vallée-Bélisle, A.; Moscone, D.; Plaxco, K. W.; Palleschi, G.; Ricci, F. *Anal. Chem.* **2010**, *82*, 9109−9115.
(36) Wang, X. Z.; Jiang, A. W.; Hou, T.; Li, F. *Anal. Chim. Acta* **2015**, *890*, 91−97.
(37) Xiong, E. H.; Zhang, X. H.; Liu, Y. Q.; Zhou, J. W.; Yu, P.; Li, X. Y.; Chen, J. H. *Anal. Chem.* **2015**, *87*, 7291−7296.
(38) Du, Y.; Lim, B. J.; Li, B. L.; Jiang, Y. S.; Sessler, J. L.; Ellington, A. D. *Anal. Chem.* **2014**, *86*, 8010−8016.
(39) Wu, L.; Zhang, X. H.; Liu, W.; Xiong, E. H.; Chen, J. H. *Anal. Chem.* **2013**, *85*, 8397−8402.
(40) Ren, K. W.; Wu, J.; Yan, F.; Zhang, Y.; Ju, H. X. *Biosens. Bioelectron.* **2015**, *66*, 345−349.
(41) Xiong, E. H.; Wu, L.; Zhou, J. W.; Yu, P.; Zhang, X. H.; Chen, J. H. *Anal. Chim. Acta* **2015**, *853*, 242−248.
(42) Dao, V.; Guenther, R. H.; Agris, P. F. *Biochem.* **1992**, *31*, 11012−11019.
(43) Ramsing, N. B.; Rippe, K.; Jovin, T. M. *Biochem.* **1989**, *28*, 9528−9535.
(44) Bardea, A.; Patolsky, F.; Dagan, A.; Willner, I. *Chem. Commun.* **1999**, 21−22.
(45) Cao, Y.; Zhu, S.; Yu, J. C.; Zhu, X. J.; Yin, Y. M.; Li, G. X. *Anal. Chem.* **2012**, *84*, 4314−4320.
(46) Grossmann, T. N.; Röglin, L.; Seitz, O. *Angew. Chem., In. Ed.* **2007**, *46*, 5223−5225.
(47) Zheng, J.; Li, J. S.; Jiang, Y.; Jin, J. Y.; Wang, K. M.; Yang, R. H.; Tan, W. H. *Anal. Chem.* **2011**, *83*, 6586−6592.
(48) Vasquez, K. M.; Glazer, P. M. *Q. Rev. Biophys.* **2002**, *35*, 89−107.
(49) Frank−Kamenetskii, M. D.; Mirkin, S. M. *Annu. Rev. Biochem.* **1995**, *64*, 65−95.
(50) Wang, J.; Cai, X. H.; Rivas, G.; Shiraishi, H.; Farias, P. A.; Dontha, N. *Anal. Chem.* **1996**, *68*, 2629−2634.
(51) Fan, Q.; Zhao, J.; Li, H.; Zhu, L.; Li, G. X. *Biosens. Bioelectron.* **2012**, *33*, 211−215.
(52) Xuan, F.; Luo, X. T.; Hsing, I. M. *Anal. Chem.* **2012**, *84*, 5216−5220.
(53) Dou, B. T.; Yang, C. Y.; Chai, Y. Q.; Yuan, R.; Xiang, Y. *Analyst* **2015**, *140*, 5981−5986.

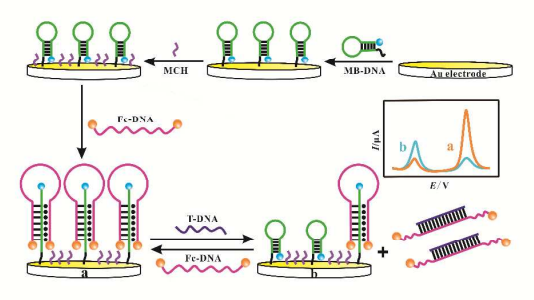

For TOC Only